Improved aromatic yield and toluene selectivity in propane aromatization over Zn–Co/ZSM-5: effect of metal composition and process conditions

G. Oseke, E. Peter, A. Atta, B. Mukhtar, B. El-Yakubu, B. Aderemi

Improved aromatic yield and toluene selectivity in propane aromatization over Zn–Co/ZSM-5: effect of metal composition and process conditions

G. G. Oseke[1] · E. E. Peter[1,3,4] · A. Y. Atta[1] · B. Mukhtar[1] · B. J. El-Yakubu[1] · B. O. Aderemi[1,2]

Abstract
In this report, a catalytic enhanced-conventional process production background was employed to determine the most cost-effective and environmentally friendly techniques to improve the catalytic production of toluene and other aromatic compounds from propane aromatization. 2 wt% of zinc was co-impregnated with 1–3 wt% of cobalt on HZSM-5. Characterizations and analysis showed that catalysts are crystalline and microporous. Propane conversion was carried out at 540 ° C, 1200 ml/g-h gas hourly space velocity and atmospheric pressure over Zn–Co/ZSM-5 bimetallic catalysts. Toluene selectivity in the aromatic products was greatly improved and sustained significantly together with other aromatic products. Catalytic conversion of propane and aromatic yield over Zn–Co/ZSM-5 was improved and stabilized due to metallic collaboration on HZSM-5. Aromatic yield averaged 46, 32, and 36%, respectively, for 1–3 wt% Co in Zn–Co/ZSM-5 bimetallic catalyst. Average toluene selectivity in the aromatic products for 12 h time on stream from 60, 50 and 51% for 1–3 wt% Co loading. The threshold loading of cobalt with zinc was 2% above which the general aromatic selectivity declined. A decrease in conversion from 73 to 15% was observed for flowrate increase from 6 to 35 ml min^{-1} and an increase in aromatic selectivity from 80 to 87%. An increase in temperature of 500–560 °C increased catalytic performance, 32–47% for propane conver-sion, and 79–86% aromatic selectivity.

Keywords Propane conversion · Aromatic yield · Toluene selectivity · Zn–Co/ZSM-5

Abbreviations

BET	Brunauer–Emmett–Teller
BTEX	Benzene toluene ethylbenzene xylene
FTIR	Fourier transform infra-red
H_2-TPR	Hydrogen-temperature programming reduction
SEM	Scanning slmctron microscopy
TEM	Transmission electron microscopy
XPS	X-ray photoelectron spectroscopy
XRD	X-ray diffraction
XRF	X-ray fluorescence

✉ G. G. Oseke
osechemtechy@gmail.com; ggoseke@abu.edu.ng

[1] Chemical Engineering Department, Ahmadu Bello University, Zaria, Nigeria

[2] Chemical Engineering Department, Landmark University, Omu-Aran, Nigeria

[3] Rapsodee Research Centre, IMT-Mines, Albi-Carmaux, France

[4] Laboratoire de Physique et Chimie des Nano-Objects, INSA, Toulouse, France

1 Introduction

Aromatic compounds which comprise benzene, toluene, and xylenes (m, o, and p,) and ethylbenzene serves as feedstocks for a good number of intermediates that are used for the manufacture of synthetic rubber dyes, explosives, pesticides, detergents, resins. etc. [1, 2] Styrene, linear alkyl benzene, and cumene are serves as the foremost consumer of benzene. These are largely in demand, making aromatic compound production to have and still attracting attention both in academic and industrial research [3–6].

Quite a lot of conventional industrial processes for the manufacture of aromatic compounds include; Carbonization of coal, naphtha steam cracking, catalytic reforming of low octane naphtha, cyclar technology of BP-UOP, naphtha dearomatization, toluene hydro-dealkylation, and toluene

disproportionation, KTI Pyroforming, Cheveron's Aromax process, Mitsubishi's Zforming process etc [7–14].

Aromatization is the catalytic process that converts light hydrocarbons to usable aromatic compounds. ZSM-5 among many other catalysts is known to be an exceptional average-sized pore zeolite making it fit for lower alkanes aromatization [15, 16]. Cracking, oligomerization, and cyclization are major reaction steps in aromatization [17, 18]. Toluene is a non-polar aromatic hydrocarbon produced mostly from petroleum which is majorly used as solvent toluene, the production of benzoic acid, chloro-toluene derivatives, trinitro-toluene (explosives), toluene sulphonic acid, toluene sulphonamide, benzaldehyde, polyurethane, toluene diisocyanate, recreational inhalant among others. Toluene is an important non-polar aromatic feedstock to petrochemical industries commercially produced alongside other aromatic compounds by carbonization of coal, steam cracking of naphtha, and catalytic reforming of low octane naphtha.

Aromatic compound production from light alkanes from previous research employed modified catalysts with impregnated mono or bimetallic as dehydrogenating agents and promoters to improve aromatic yield and selectivity as HZSM-5 has a low aromatic yield. Zn, Ga, and Pt among many metals have emerged as outstanding at dehydrogenation. The economy of procurement is of advantage with the use of Zn with no health concern but unstable at reaction condition. HZSM-5 and other metal-modified catalysts (mono and bi) have been used in aromatization in previous research. Cr was impregnated with Ga/ZSM-5 which increased the dehydrogenation step of the aromatization in which Cr inhibited dispersion which could no longer promote propane conversion and overall aromatic yield [19]. The promotional Effect of CO_2 on propane aromatization over Zn/ZSM-5 was studied alongside the addition of second metal to eradicate carbon deposit on the catalyst thus enhancing catalyst stability [20]. Zn–Ni/ZSM-5 was used for catalytic aromatization of olefin/paraffin which showed improved aromatic selectivity [21]. Propane was converted to liquid hydrocarbons using Pt-Zn/SiO2 + ZSM-5. Catalyst performed better at high temperatures, improved aromatic selectivity, and alteration of reaction pathways due to changes in temperature [22]. Lanthanum/Gallium-Modified Zn/ZSM-5 Zeolite was used to investigate the isomerization/aromatization of FCC Light Gasoline which revealed that La and Ga aided the dispersion of Zn thus enhancing the isomerization/aromatization activities and prolonging the service life of the catalysts [23]. Ga and Zn/ ZSM-5 were used for the conversion of LPG to Aromatics in which Ga showed better performance according to the industrial feed [24].

General improved selectivity had been reported but not tailored selectively towards toluene production [25–29]. Due to the increasing demand and use of toluene in petrochemical industries as feedstocks for benzene and other petrochemical products, there is a need to develop stable bimetallic catalysts highly selective towards toluene production owing. Through this investigation, we report efficient stable and toluene-selective catalysts having an unaltered reaction pathway for propane aromatization and overall improved aromatic selectivity.

2 Experimental procedures

2.1 Preparation of catalysts

Zn–Co/ZSM-5 catalyst was prepared using NH_4-ZSM-5, hydrates of $Zn(NO_3)_2$ and $(Co(NO_3)_2$ by the wet co-impregnation method employed in our previous studies [26–28].

2.2 Characterization of catalysts

FTIR, FTIR-pyridine, XRD, BET, and textural properties, SEM, TEM, hydrogen-TPR, and XPS were employed in catalyst characterization as reported in our earlier studies procedures [26–28].

2.3 Catalytic activity test

Aromatization propane was carried out using already established procedures in our previous research on stainless-steel fixed bed reactor with propane (C_3) conversion and product selectivity calculated using the same equations [26–28].

3 Results and discussions

FTIR spectra in Fig. 1 show the presence of peak spectra of characteristic functional groups of Zn–Co/ZSM-5. 450 and 550 cm^{-1} peaks that appeared depict T-O bending and crystalline double-5 ring of ZSM-5. 1100 and 1225 cm^{-1} peaks match to inner and outer asymmetric stretch respectively [26–29]. Broader and wider were observed with an increase in metal loading showing metallic bond stretching. 3400 and 1700 cm^{-1} match the stretch and vibrational bend of the OH^- group of absorbed water on the surface of H-ZSM-5 [29–31].

XRD of Zn–Co/ZSM-5 catalysts are presented in Fig. 2 which demonstrated their lattice structures. From our previous studies, there were slight decreases in the intensities of characteristic diffraction peaks as metal dosage on ZSM-5 increased because of metal deposition on zeolite pores and surface [32–35]. The surface metal modification did not affect catalysts' crystallinity as there was no collapse or alteration of structure [8, 32–35]. There was no distinct characteristic peak and mismatch in the diffractogram or new phase formations on bimetallic Zn–Co/ZSM-5

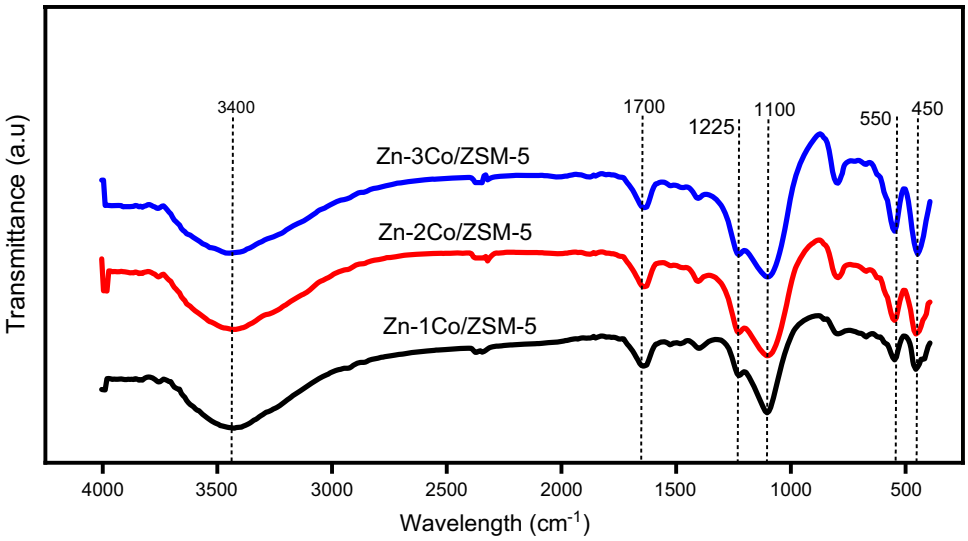

Fig. 1 FTIR-spectra of Zn–Co/ZSM-5 catalysts

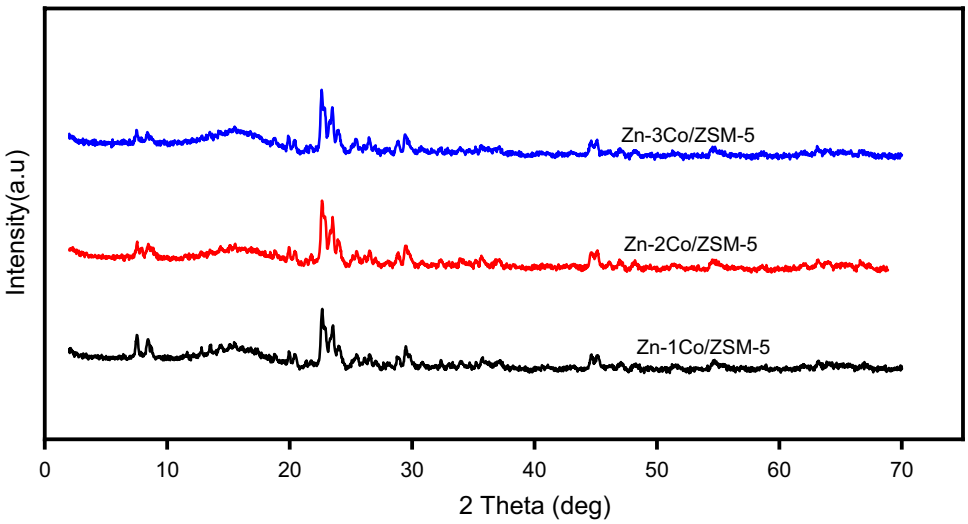

Fig. 2 X-ray diffractogram of Zn–Co/ZSM-5

because of low metal dosage [36, 37]. The observed typical peaks of HZSM-5 appeared for all modified catalysts at 2θ angle = 7.89°, 8.73°, 14.82°, 23.04°, 23.86°, and 24.26° [38–41].

Figure 3 show the pyridine-IR of Zn–Co/ZSM-5 catalysts. Three distinguishing peaks about 1450,1550 and 1510 cm^{-1} were detected in the catalysts though there were little shifts which characterize the amount of Lewis, Bronsted and additive Bronsted and Lewis acid sites [26, 27]. Lewis acid sites improve dehydrogenation and aromatization process. There was an increase in peak 1450 cm^{-1} corresponding to Lewis showing the effect of metal to increase Lewis acid sites and reduced Bronsted acidity [39, 42, 43].

Figure 4 show the surface morphology of zeolite catalysts from parent HZSM-5 (A) to metal impregnated catalysts Zn/ZSM-5 (B) and Zn–Co/ZSM-5 respectively of the same magnifications. Figure 4. Slight surface morphological changes were observed on modified catalysts due to impregnation of heavy metal zinc and cobalt on HZSM-5 [26–29, 44].

The transmission emission micrograms (TEM) are presented in Fig. 5 for parent HZSM-5, monometallic Zn/ZSM-5 and bimetallic Zn–Co/ZSM-5 (2 wt% each for the metals) at same resolutions. Catalyst surface voids were filled with impregnated metals when related to parent protonated ZSM-5 as the surface became finer [26–29, 44].

Table 1 presents the textural features of ZSM-5 catalysts. They all displayed Type-I N_2-isotherms deprived of distinct hysteresis loops owing to their uniform microporosity despite surface metal impregnation as shown in Fig. 6. Zn on HZSM-5 had an effect surface area reduction in relation to HZSM-5, displaying reduced microporosity and mesoporosity as a result of ZnO particles deposits on the surface by pore blockages on HZSM-5 openings as reported in our

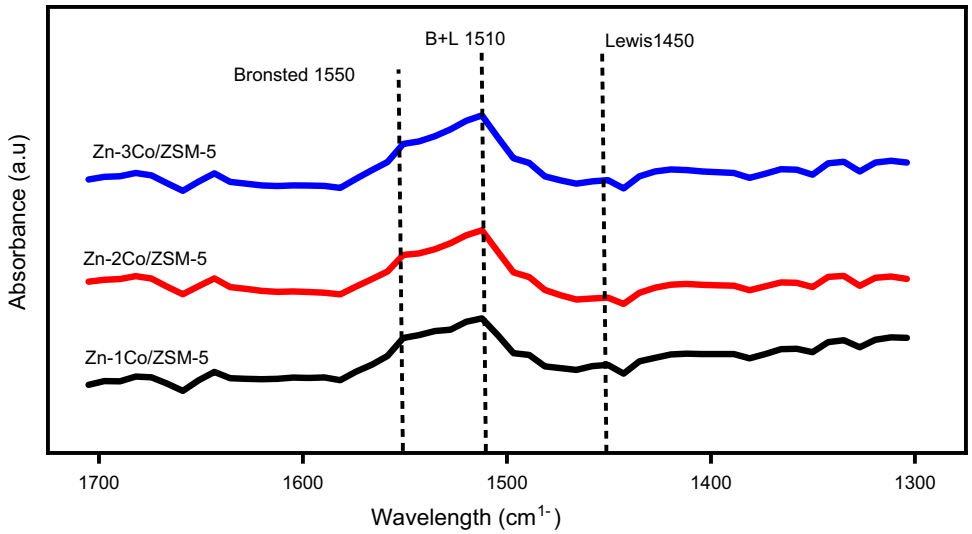

Fig. 3 Pyridine-FTIR of Zn–Co/ZSM-5 catalysts

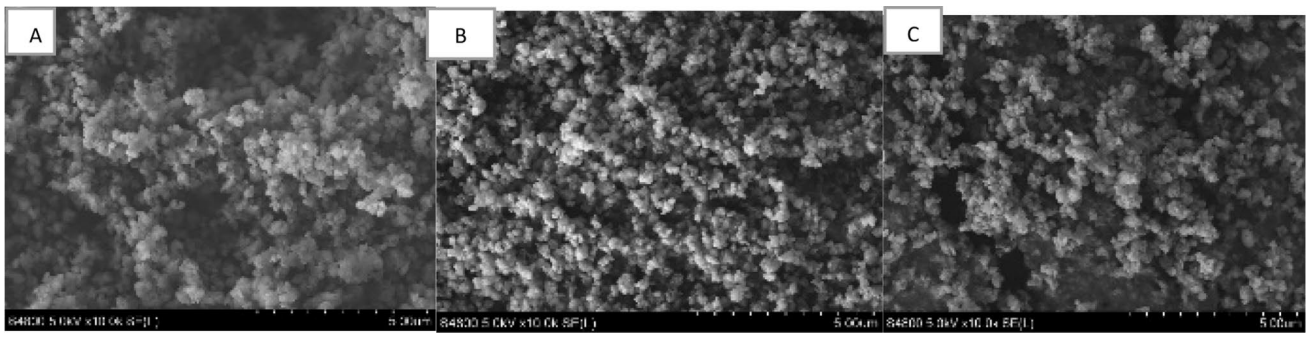

Fig. 4 Scanning micrograph of **A** (HZSM-5), **B** (Zn/ZSM-5) and **C** (Zn–Co/ZSM-5)

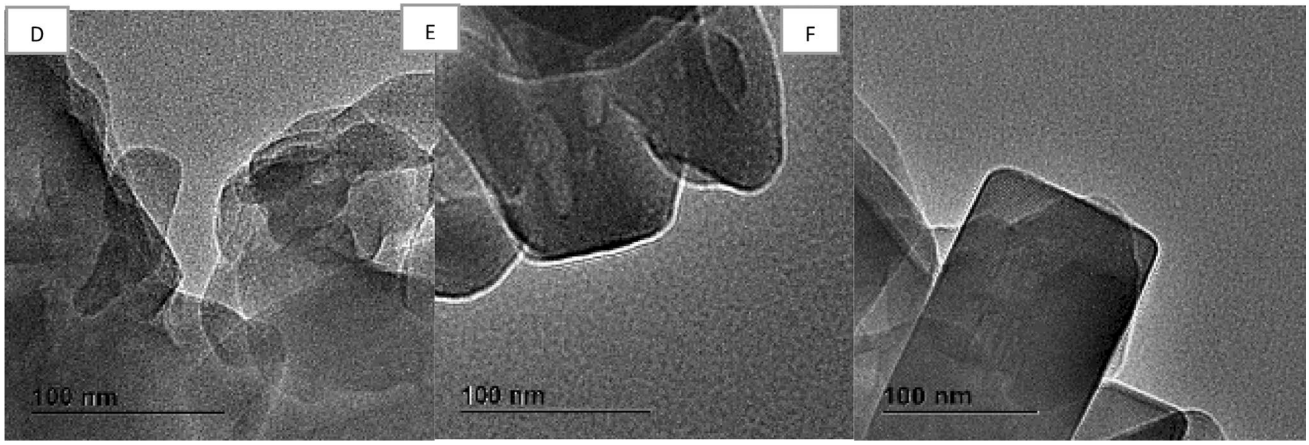

Fig. 5 Transmission micrograph of **D** (HZSM-5), **E** (Zn/ZSM-5) and **F** (Zn–Co/ZSM-5)

previous studies [26–29]. On co-impregnation of Zn with Co on the HZSM-5 catalyst, there was a reduction in the areas of micro and mesopore on account of blockage. This could be accounted for by metal particles' penetration inside the micropores, while others were available on the external surface which led to a decrease in both micropores and external surface areas. An increase in metal loading decreased total pore volume [30, 35, 36, 45]. The XRD peaks reduction of

the catalysts as metals were impregnated in Fig. 2 supported these surface properties [46, 47].

Zinc-modified zeolite and hydrogen-ZSM-5 have the same TPR plot trend as presented in our previous research in Fig. 7 under the experimental conditions showing that Zn was not reduced by hydrogen on ZSM-5 [31]. The Peak reduction for cobalt on ZSM-5 as reported by Dao et al., 2015 is 335 °C. Zn–Co/ZSM-5 showed a little shift in hydrogen consumption at around 340, 400, and 600 °C. It was reported that metal-metal interactions cause peak shifts either from the normal single metal thereby promoting the formation of stable zinc species and good electronic intermetallic interactions [26, 27, 46, 47]. The charge relocation moves the electrons from zinc and co-impregnated cobalt [48–50].

The XPS survey spectra in Fig. 8 show that the deposited metals were on the surface of ZSM-5 and the metals did not affect the entire survey spectra except for the characteristic peaks of zinc and zinc-cobalt denoting their presence on HZSM-5. XPS showed that Zn and Co both possessed

Table 1 Textural properties of Zn–Co/ZSM-5 catalysts

Catalyst(s)	S_{BET}a (m^2/g)	S_{micro}c (m^2/g)	S_{mesoc} (m^2/g)	V_{total}b (cm^3/g)	V_{micro}c (cm^3/g)	Pore width (nm)
Zn-1Co/ZSM-5	358.34	324.71	34.64	0.25	0.15	2.77
Zn-2Co/ZSM-5	359.19	324.45	34.73	0.25	0.15	2.74
Zn-3Co/ZSM5	362.02	324.72	37.30	0.25	0.15	2.72

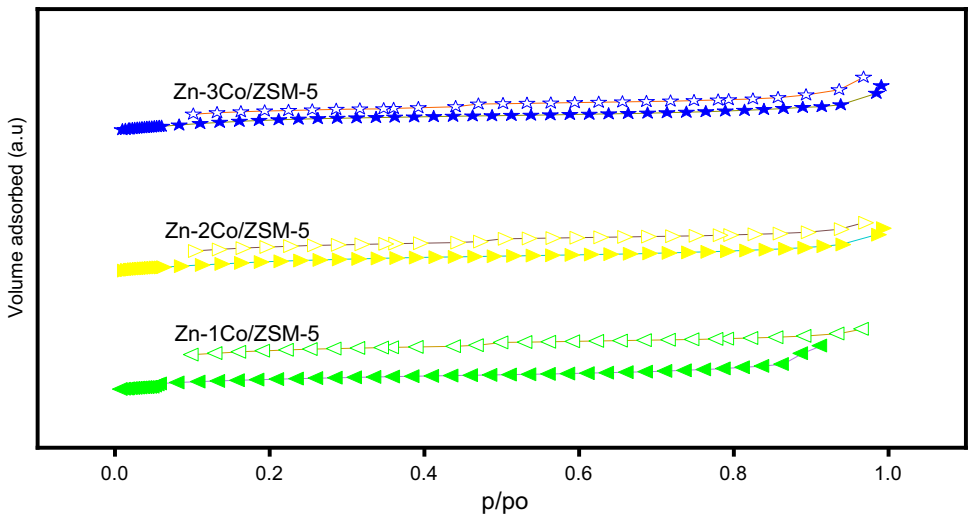

Fig. 6 N_2-adsorption of Zn–Co/ZSM-5 catalysts

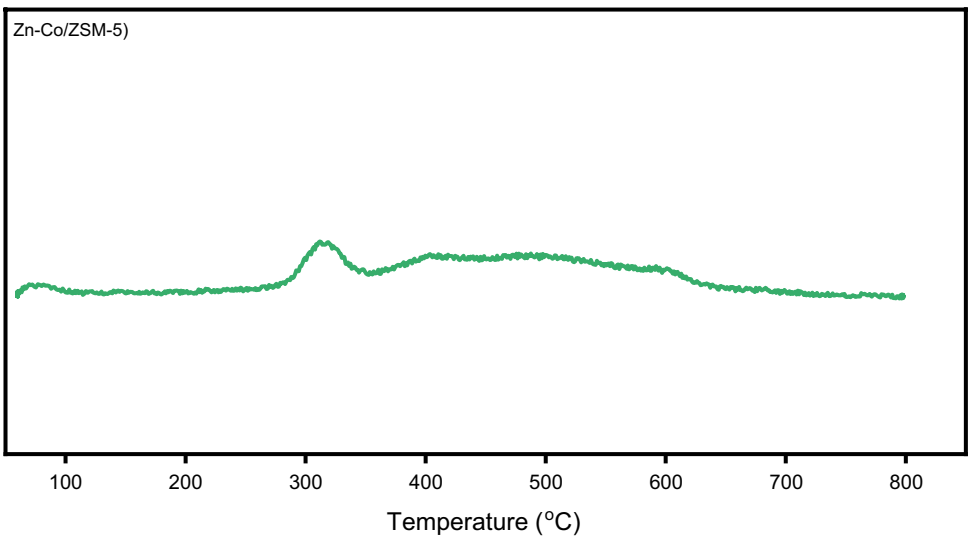

Fig. 7 Hydrogen-TPR of Zn–Co/ZSM-5 catalysts

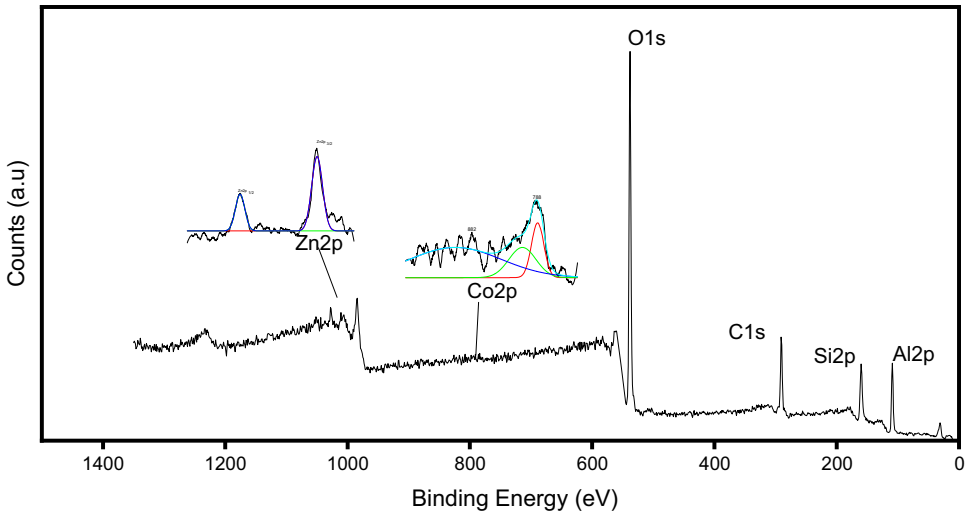

Fig. 8 XPS spectra of Zn–Co/ZSM-5 catalyst

oxidation state of 2+. Increase in metal binding energies showed zinc-cobalt interaction which had enhanced stability of zinc. Reduction binding energy of Zn $2p_{3/2}$ showed dispersion of ZnO clusters over zeolite surface while that of Zn $2p_{1/2}$ was credited to presence of $ZnOH^+$ species [31, 38]. Co loading ($Cop_{3/2}$ 788 eV) improved the distribution of ZnO and the concentration of $ZnOH^+$ which promoted alkane aromatization and suppressed the formation of light olefins [46]. The shift in the binding energies of Zn and Co (780 and 796 eV) lower and higher energy level from their oxides on zeolite are attributed to inter-metallic bonding and electron balancing on ZSM-5 [27–29].

Figures 9 and 10 show propane conversion and aromatic yield on ZSM-5 catalysts. Dehydrogenation as an important reaction step in aromatization occurs in; carbonium ion to carbenium ion and finally to small alkenes, higher olefins to di-olefins; cyclization of di-olefins to cyclic olefins and dehydrogenation of cyclic olefins to cyclic di-olefins and finally to aromatics. HZSM-5 catalyst had low selectivity owing high cracking due to beta-scission as reported in our previous studies [25–29, 37]. This occurred from reaction of surface hydrogen from hydride transfer step reacting back with alkene to form light alkanes and cyclohexane. The presence of Co with Zn on HZSM-5 helped in improving propane conversion and catalytic activity as presented in Fig. 9. Propane conversion was sustained for twelve hours of time on stream through Zn–Co interaction synergy and electron mobility on zeolite. The higher activity in propane conversion after the co-impregnation of Zn and Co 1 and 3 wt% was attributed to enhanced dehydrogenation activity of Zn by Co on HZSM-5 channels and improved stability of Zn at reaction temperature. This was clearly shown in XPS and H_2-TPR by increased binding energy and reduction temperature respectively as a result of interaction between the Zn and Co species. However, 2 wt% equal metal loading of Zn and Co had lower conversion, this was observed in our previous studies for other bimetallic catalyst.

Aromatic yield of bimetallic catalyst with varying cobalt loading co-impregnated with zinc on ZSM-5 catalysts are shown in Fig. 10. The synergy of co-impregnated metal

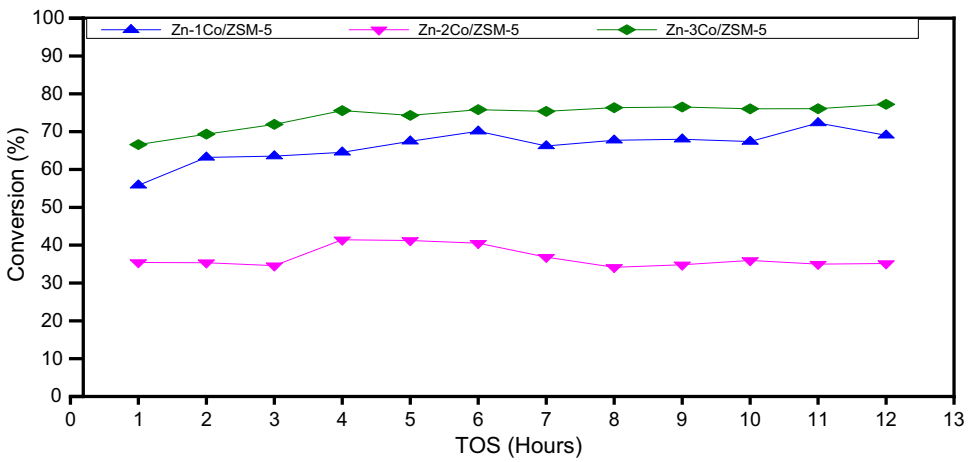

Fig. 9 Propane conversion over bimetallic Zn–Co/ZSM-5 catalysts

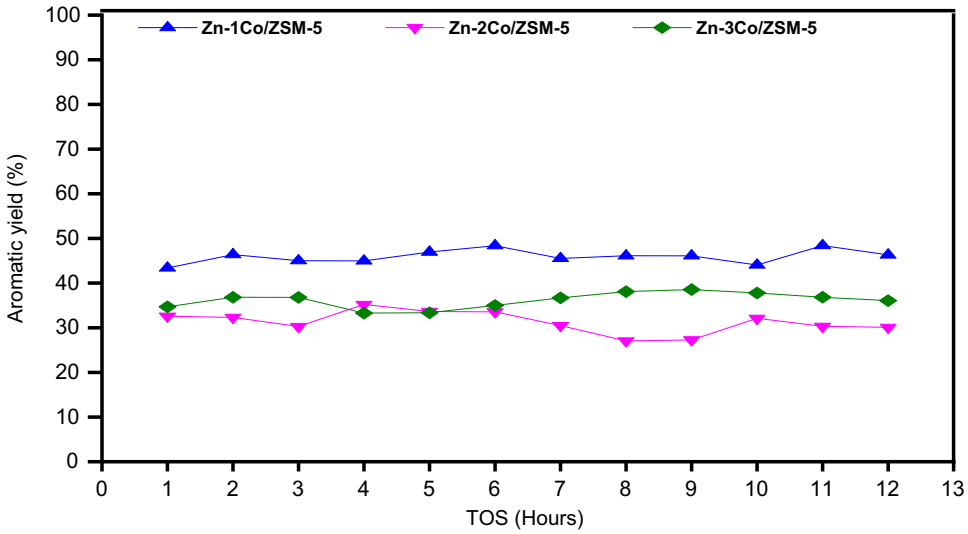

Fig. 10 Aromatic yield over bimetallic Zn–Co/ZSM-5 catalysts

species improved aromatic yield when compared with parent and Zn/ZSM-5 in the previous studies resulting from the recombination of surface generated hydrogen during hydride transfer process [25]. This suppressed cracking, minimized hydrogenation backward reaction and enhanced oligomerization and cyclization for twelve hours' time on stream [25–29, 51–53]. Zn–Co/ZSM-5 bimetallic catalyst with Co as second metal had lower conversion compared with other bimetallic catalyst. Same observations were recorded for equal metal loading bimetallic catalysts of equal 2 wt% loading of Fe, Cu and Ni as second metal with zinc on zeolite.

Performance test over ZSM-5 catalysts as earlier reported had high percentage of light gases because of surface hydrogen from hydride transfer reaction with alkene to form alkanes thereby leading to cracking and formation of cyclohexane and heptane (C_6–C_7) [32, 52–55]. Zn high dehydrogenating ability was reported as there was a boost in the aromatic compound selectivity as a result of minimized cracking and side reactions. Lighter alkanes, propene and C_{9+} components increased showing loss of Zn active site due to its instability at reaction temperature [26–29]. Further co-impregnation as experimented in this studies of Co with Zn helped to stabilize zinc thus improving and sustaining aromatic selectivity with toluene being the highest as compared to Zn/ZSM-5. Toluene was the most stable among the aromatic compound because of the methyl-group as electron donor to the benzene ring. Presence of cobalt aided alkylation of benzene and demethylation of xylene to

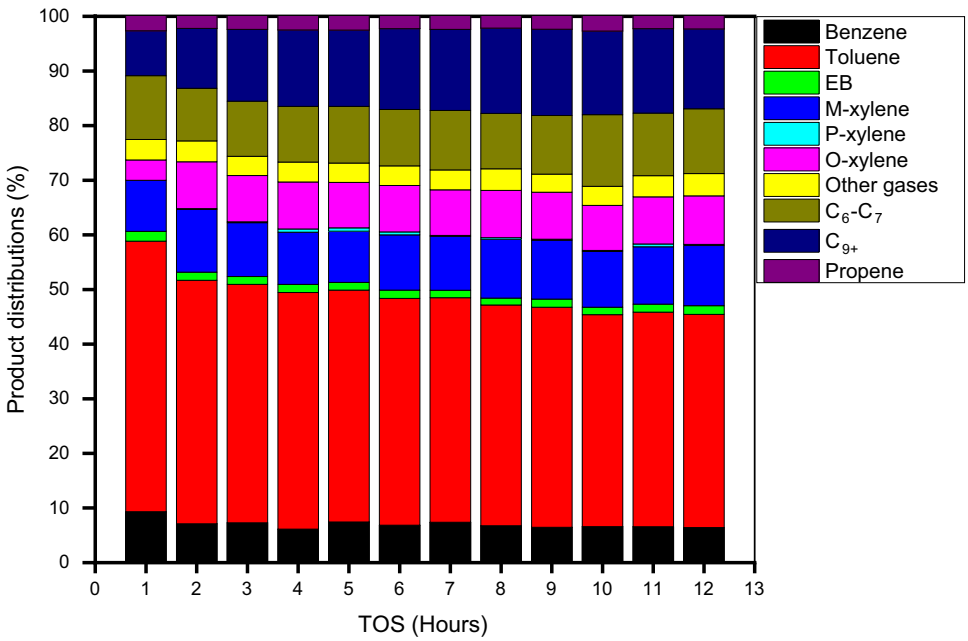

Fig. 11 Product distribution and aromatic selectivity over Zn-1Co/ZSM-5

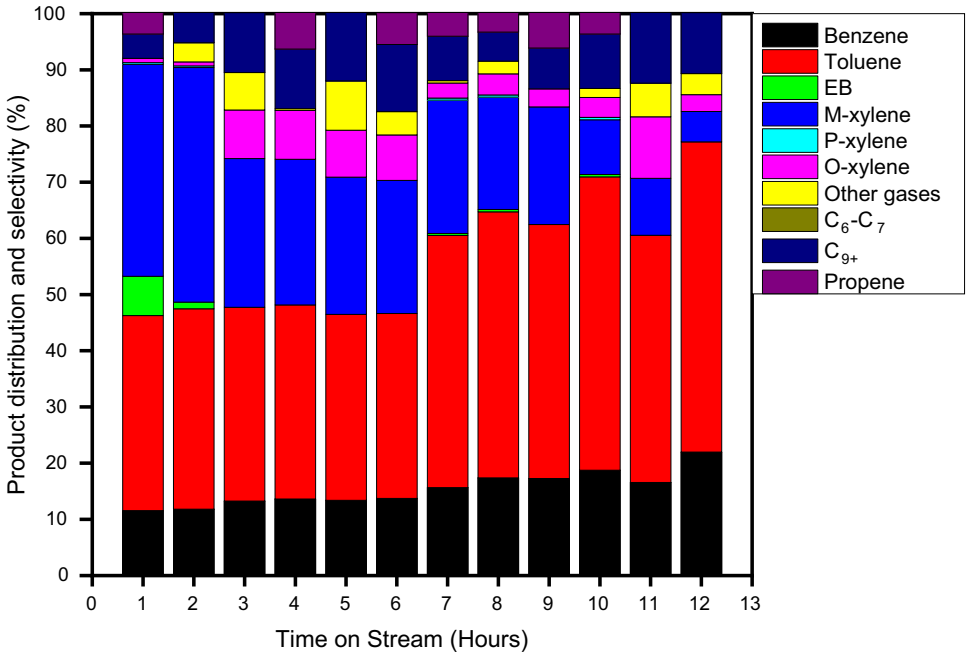

Fig. 12 Product distribution and aromatic selectivity over Zn-2Co/ZSM-5

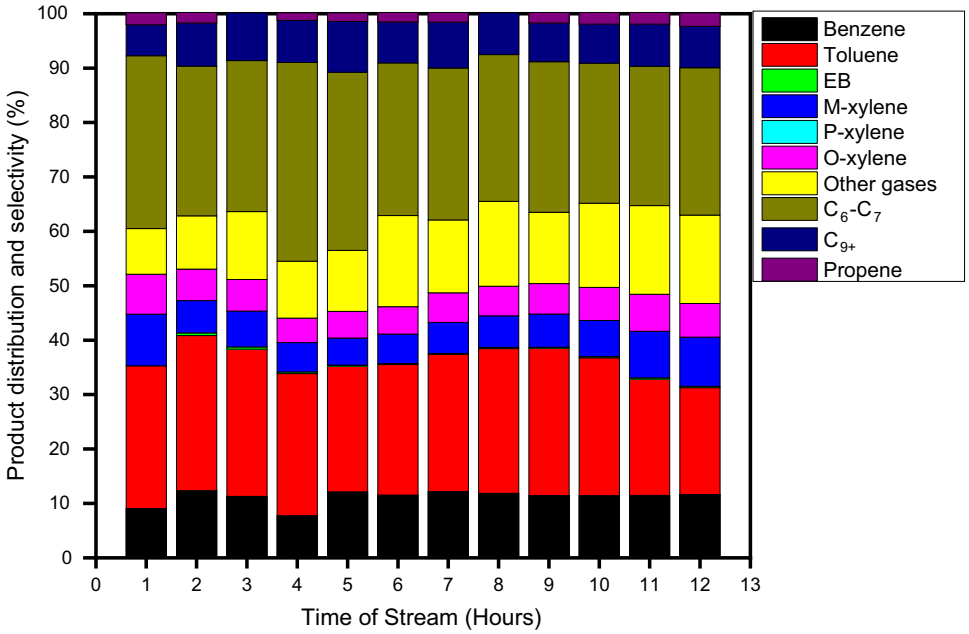

Fig. 13 Product distribution and aromatic selectivity over Zn-3Co/ZSM-5

form more of toluene as was clearly observed in Figs. 11, 12 and 13 with improved and stable selectivity. Aromatic selectivity with 1 wt% Co with Zn on ZSM-5 in Fig. 11 had lighter gases, cyclohexane, heptane and with reduced C_{9+} when compared already reported Zn/ZSM-5. Cobalt presence prevented build-up of higher aromatics. Toluene selectivity in Zn–Co/ZSM-5 catalysts reduced as cobalt loading increased. Aromatization with 1 wt% of Co with Zn on ZSM-5 produced more toluene, lesser benzene and m-xylene among other aromatic products with more cyclohexane and C_{9+} as compared other catalysts' performance test. Equal 2 wt% of Co and Zn yielded toluene, benzene and m-xylene among other aromatic products with lower minimal light gases, cyclohexane, heptane and C_{9+}. Propane conversion on 3 wt% of Co with Zn had reduced aromatic yield forming more of light alkanes, cyclohexane and light alkanes in the

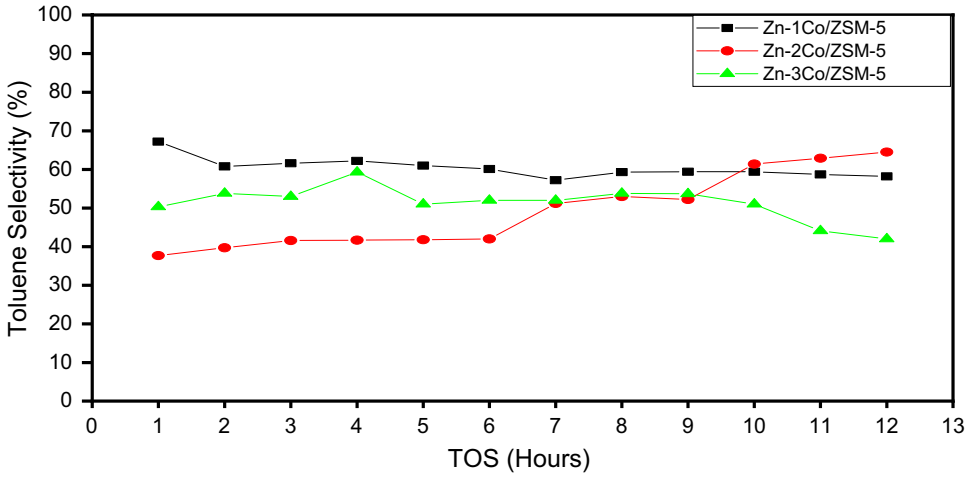

Fig. 14 Toluene selectivity in the aromatic products over Zn–Co/ZSM-5 catalysts

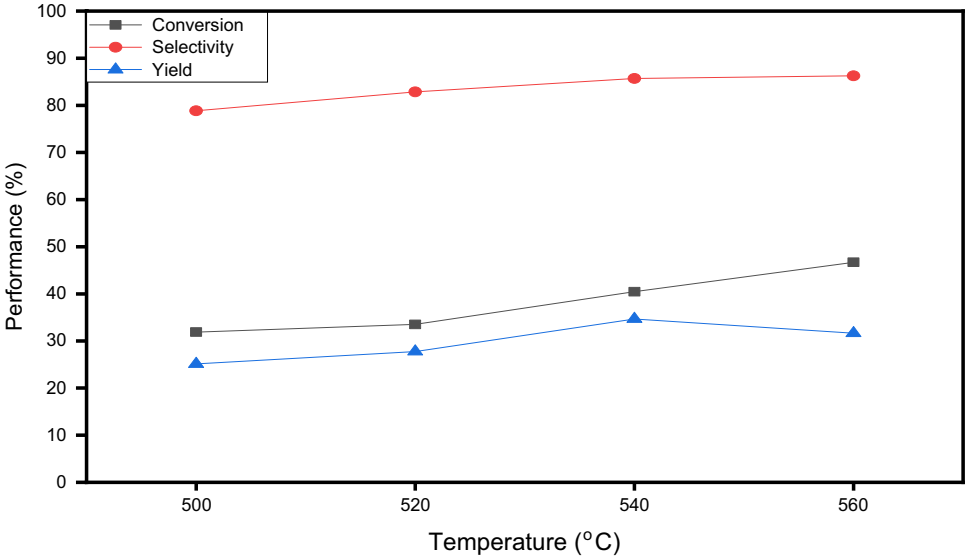

Fig. 15 Effect temperature on catalytic performance

aromatic product distribution. This would have resulted from the coverage active sites for dehydrogenation thus cracking set in as observed in Fig. 11.

Figure 14 shows the toluene selectivity in the aromatic products for twelve hours' time on stream for 1–3 wt% cobalt co-loading with 2 wt% zinc on ZSM-5 catalyst. It was observed that 1 wt% cobalt had sustained toluene selectivity of 65% while 2 wt% of cobalt was on the increase from 35 to 70%. 3 wt% had light gases and hexanes which are not desired.

3.1 Effect of temperature and feed flow rate on propane aromatization over Zn–Co/ZSM-5

Process condition performance test were carried out for 2 wt% Zn with 2 wt% Co on ZSM-5 being the best performed catalyst with respect to aromatic selectivity and increased toluene content in the aromatic product.

Figure 15 shows the effect of temperature on catalytic performance. Aromatization is an endothermic reaction and the energy-demanding process makes temperature an important process condition. Temperature from 500 to 580 °C favour catalytic performance as it enhances dehydrogenation, oligomerization and cyclization with both increase in propane conversion and aromatic selectivity [30, 48, 56]. It can be seen that C_{9+} cracked to lower aromatics which were clearly seen in toluene, benzene, o and m-xylene increase in Fig. 16. Demethylation and methylation processes were observed to be happening concurrently with variation increase in one aromatic compound leading to a decrease in another.

Figures 17 and 18 show the effect of increase in propane flow rate on catalytic performance and product distribution

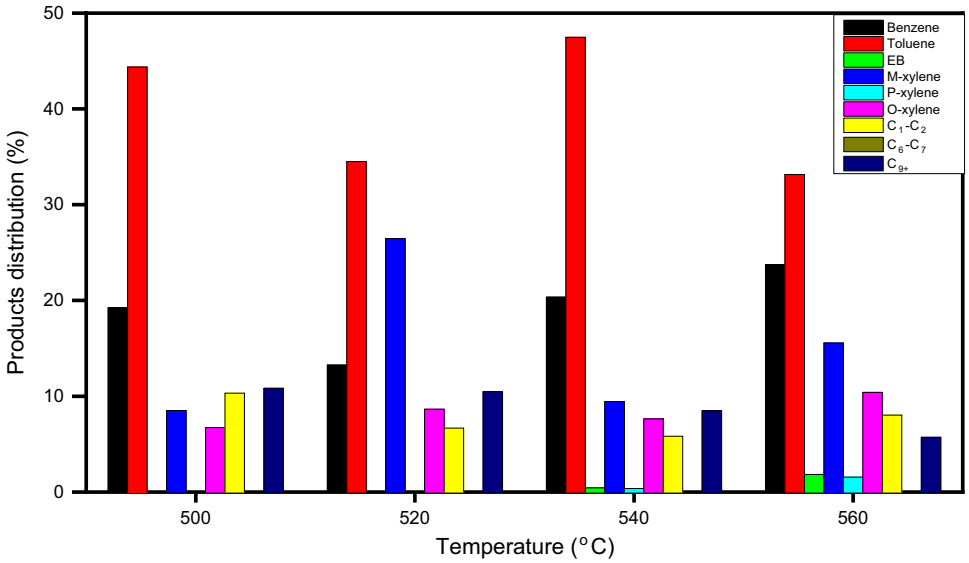

Fig. 16 Effect temperature on product distribution

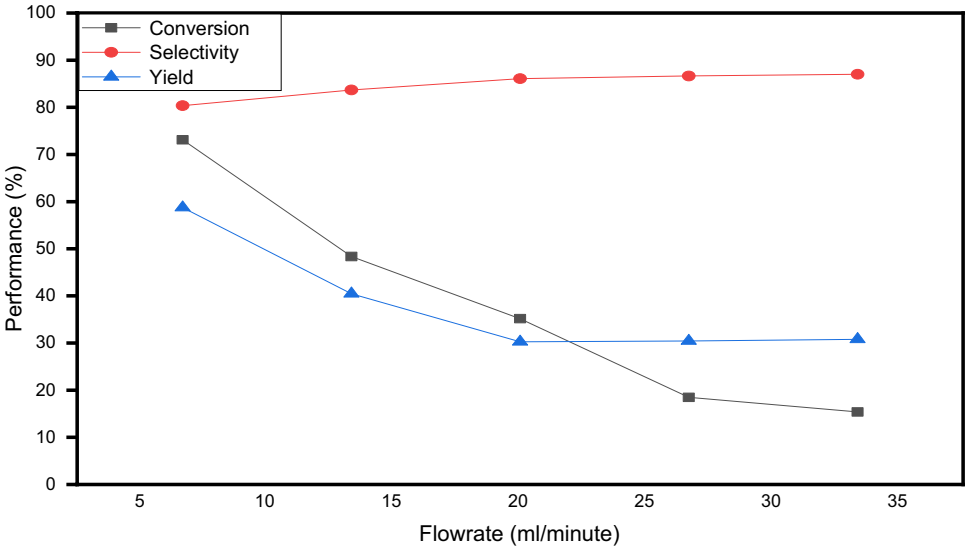

Fig. 17 Effect feed flow rate on catalytic performance

respectively. Propane shorter time of contact with the surface of the catalyst reduced led to a reduction in the conversion with an increase from 6 to 35 ml min^{-1} (29). An increase in feed rate improved aromatic selectivity as the C_{9+} build-up time of higher aromatics was limited [25]. Figure 18 showed the product distribution as C_1-C_3 gases were reduced because more of lighter hydrocarbons were consumed during benzene alkylation to toluene and other xylenes. Benzene was fairly steady among the aromatic compounds while toluene selectivity was on the increase. The effect of flowrate increase was observed in the toluene increase resulting from decrease in C_{9+} because of limited build-up time for higher aromatics formation, thus an overall increase in aromatic selectivity.

4 Conclusion

Propane was aromatized catalytically over Zn–Co/ZSM-5 bimetallic catalysts. The performance test showed that the catalyst is stable and promotes aromatic compound formation and of high selectivity toward toluene. The characterization techniques employed showed crystallinity and structure zeolite retained despite impregnation of metals. Synergy of cobalt with zinc improved and sustained catalyst activity and over all aromatic selectivity especially toluene among other aromatic compounds.

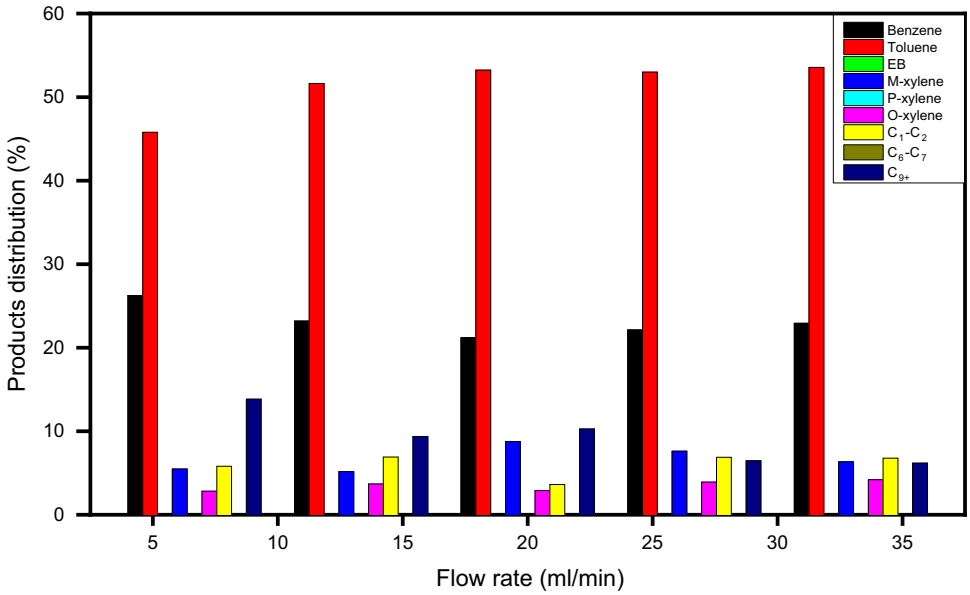

Fig. 18 Effect feed flow rate on product distribution

Acknowledgements A deep appreciation from the authors goes to the Petroleum Technology Development Fund (PTDF), Abuja, Nigeria for providing support and funding for this research.

Author contributions All authors were involved in the manuscript proofreading but below are the unique contributions of an individual with the corresponding author, Dr. Oseke Godwin Gbenga carried out the research in the laboratory and prepared the manuscript. Professor AAY was deeply involved in catalyst synthesis and effective operations of the fixed bed reactor. Professor MB and Professor EYBJ contributed to catalyst performance tests in relation to characterization. Professor ABO contributed to catalyst characterization, understanding the reaction mechanism in relation to performance tests, and general organization of the research. EEP contributed to understanding the reaction mechanism, temperature effect on product distribution, and metal catalyst interactions.

Funding This research was funded by Petroleum Technology Development Fund, PTDF, Ministry of Petroleum Resources, Abuja-Nigeria.

Data availability All data generated or analysed during this study are included in this published article and are provided in the supplementary information files.

Declarations

Conflict of interest The authors of this paper declare that we have no known competing financial interests or personal relationships that could have appeared to influence the work reported in this paper.

References

1. B. Liu, S. Lu, E. Liu, X. Hu, J. Fan, Korean J. Chem. Eng. **35**(4), 867–874 (2018)
2. B.S. Kwak, W.M. Sachtler, Korean J. Chem. Eng. **13**(4), 356–363 (1996)
3. Y.K. Park, D.H. Kim, S.I. Woo, Korean J. Chem. Eng. **14**(4), 249–256
4. X. Chen, M. Dong, X. Niu. K. Wang, G. Chen, W. Fan, Z. Qin, Chin. J. Catal. **36**(6), 880–888 (2015)
5. J. Park, W.Y. Lee, H.S. Hahm, Korean J. Chem. Eng. **19**(3), 411–416 (2002)
6. T. Yang, L. Cheng, N. Li, D. Liu, Ind. Eng. Chem. Res. **56**(41), 11763–11772 (2017)
7. D. Bhattacharya, S. Sivasanker, J. Catal. **153**(2), 353–355 (1995)
8. Y. Xu, L. Liwu, Appl. Catal. A **188**(1–2), 53–67 (1999)
9. I.D. Mall, *Petrochemical Process Technology*, 1st edn. (New Delhi, Macmillan India, 2007)
10. K. Frey, L.M. Lubango, M.S. Scurrell, L. Guczi, Reaction Kinetics, Mechanisms and Catalysis **104**(2), 303–309 (2011)
11. C. Song, K. Liu, D. Zhang, S. Liu, X. Li, S. Xie, L. Xu, Appl. Catal. A **470**, 15–23 (2014)
12. M. Miyamoto, K. Mabuchi, J. Kamada, Y. Hirota, Y. Oumi, N. Nishiyama, S. Uemiya, J. Porous Mater. **22**(3), 769–778 (2015)
13. M.S. Pereira, M.S. Alexander, A. Marco, N. Chaer, J. Phys. Chem. C **115**(20), 10104–10113 (2011)
14. S.M. Csicsery, Shape-selective Catalyst in Zeolite. Zeolite, Vol. 4, Issue 3, 202–213. 1984
15. H. Jiang, M.S. Tzou, W.M.H. Sachtler, Appl. Catal. **39**, 255–265 (1988)
16. M. Guisnet, N.S. Gnep, D. Aittaleb, Y.J. Doyemet, Appl. Catal. A **87**(2), 255–270 (1992)
17. N. Viswanadham, G. Muralidhar, T.S.R.P. Rao, J. Mol. Catal. A **223**, 269–274 (2004)
18. S. Phatanasri, P. Praserthdam, A. Sripusitto, Korean J. Chem. Eng. **17**(4), 409–413 (2000)
19. B. Xu, M. Tan, X. Wu, H. Geng, S. Zhao, J. Yao, et al., Propane aromatization tuned by tailoring Cr Modified Ga/ZSM-5 catalysts. ChemCatChem **13**(16), 3601–3610 (2021)
20. H. Fan, X. Nie, C. Song, X. Guo, *Mechanistic Insight into the Promotional Effect of CO2 on Propane Aromatization over Zn/ZSM-5* (Industrial & Engineering Chemistry Research, 2022)
21. T. Pan, S. Ge, M. Yu, Y. Ju, R. Zhang, P. Wu, … Z. Wu, Synthesis and consequence of Zn modified ZSM-5 zeolite supported Ni catalyst for catalytic aromatization of olefin/paraffin. Fuel **311**, 122629 (2022)
22. C.W. Chang, J.T. Miller, Catalytic process development strategies for conversion of propane to liquid hydrocarbons. Appl. Catal. A **643**, 118753 (2022)

23. S. Song, T. Li, Y. Ju, Y. Li, Z. Lv, P. Zheng, et al., Lanthanum/gallium-modified Zn/ZSM-5 zeolite for efficient isomerization/aromatization of FCC light gasoline. Ind. Eng. Chem. Res. **61**(27), 9667–9677 (2022)
24. S. Hajimirzaee, S. Mehr, A., & E. Kianfar (2020). Modified ZSM-5 zeolite for conversion of LPG to aromatics. Polycyclic Arom. Compd. 1–14
25. I.B. Dauda, M. Yusuf, S. Gbadamasi, M. Bello, A.Y. Atta, B.O. Aderemi, B.Y. Jibril, ACS Omega (2020)
26. G.G. Oseke, A.Y. Atta, M. Bello, J.B. Yakubu, B.O. Aderemi, Appl. Petrochem. Res. **10**(2), 55–65 (2020)
27. G.G. Oseke, A.Y. Atta, M. Bello, J.B. Yakubu, B.O. Aderemi. J. King Saud Univ. Eng. Sci. **33**, 531–538 (2021)
28. G.G. Oseke, A.Y. Atta, M. Bello, J.B. Yakubu, B.O. Aderemi, NSChE J. **35**(1), 17 (2020)
29. G.G. Oseke, A.Y. Atta, M. Bello, J.B. Yakubu, B.O. Aderemi. J. Porous Mater. https://doi.org/10.1007/s10934-022-01294-2 (2022)
30. J. Liu, G. Jiang, Y. Liu, J. Di, Y. Wang, Z. Zhao, J. Liu, Sci. Rep. **4**, 7276 (2014)
31. R. Sabarish, G. Unnikrishnan, SN Appl. Sci. **1**(9), 989 (2019)
32. B. Liu, S. Lu, E. Liu, X. Hu, Fan, J. Korean J. Chem. Eng. **35**(4), 867–874 (2018)
33. J. Park, W.Y. Lee, H.S. Hahm, Korean J. Chem. Eng. **19**(3), 411–416 (2000)
34. Y. Jia, J. Wang, K. Zhang, W. Feng, S. Liu, C. Ding, P. Liu, Microporous Mesoporous Mater. **247**, 103–115 (2017)
35. V. Ramasubramanian, D.J. Lienhard, H.G.L. Ramsurn, G.L. Price, Catal. Lett. **149**(4), 950–964 (2019)
36. W. Zhou, J. Liu, J. Wang, L. Lin, X. Zhang, N. He, H. Guo, Catal. Lett. **149**(8), 2064–2077 (2019)
37. Y. Xin, P. Qi, X. Duan, H. Lin, Y. Yuan, Catal. Lett. **143**(8), 798–806 (2013)
38. B.K. Van der, V.V. Galvita, G.B. Marin, Appl. Catal. A **492**, 117–126 (2015)
39. W. Wannapakdee, D. Suttipat, P. Dugkhuntod, T. Yutthalekha, A. Thivasasith, P. Kidkhunthod, C. Wattanakit, Fuel **236**, 1243–1253 (2019)
40. S.H. Zhang, Z.X. Gao, S.J. Qing, S.Y. Liu, Y. Qiao, Chem. Pap. **68**(9), 1187–1193 (2014)
41. X. Niu, J. Gao, Q. Miao, M. Dong, M.G. Wang, W. Fan, J. Wang, Microporous Mesoporous Mater. **197**, 252–261 (2014)
42. X. Wang, J. Zhang, T. Zhang, H. Xiao, F. Song, Y. Han, Y. Tan, RSC Adv. **6**(28), 23428–23437 (2016)
43. E. Mannei, F. Ayari, E. Asedegbega-Nieto, M. Mhamdi, G. Delahay, Z. Ksibi, A. Ghorbel, Chem. Pap. **73**(3), 619–633 (2019)
44. A.K. Mageed, A.D. Radiah, A. Salmiaton, S. Izhar, M.A. Razak, J. King Saud Univ. Sci. **31**(4), 878–885 (2019)
45. W.W. Fang, M.M. Mu, J. Tian, L.G. Chen, Y. Li, Chem. Pap. **70**(4), 430–435 (2016)
46. T.K.T. Dao, C.L. Luu, Nanosci. Nanatechnol. **6**(3), 035014 (2015)
47. Y.C. Yang, H.S. Weng, J. Mol. Catal. A **304**(1–2), 65–70 (2009)
48. J. Jarvis, P. He, A. Wang, H. Song, Fuel **236**, 1301–1310 (2019)
49. J. Jarvis, A. Wong, P. He, Q. Li, H. Song, Fuel **223**, 211–221 (2018)
50. M. Roy, G. Sourav, K.N. Milan, Mater. Chem. Phys. **159**, 101–106 (2015)
51. S.H. Zhang, Z.X. Gao, S.J. Qing, S.Y. Liu, Y. Qiao, Chem. Pap. **68**(9), 1187–1193
52. M.S. Scurrell, Appl. Catal. **41**, 89–98 (1988)
53. T.E. Tshabalala, M.S. Scurrell, Catal Commun. **72**, 49–52 (2015)
54. Y. Xu, S. Yoshizo, Z. Zhan-Guo, Appl. Catal. A **452**, 105 (2013)
55. X. Zhu, H. Wang, G. Wang, Y. Hou, J. Zhang, C. Li, C. Yang, J. Porous Mater. **28**(4), 1059–1067 (2021)
56. E.E. Peter, A.Y. Atta, B. Mukhtar, B.O. Aderemi, B.J. El-Yakub, J. King Saud Univ. Eng. Sci. **33**(7), 447–458 (2021)